Int. J. Electrochem. Sci., 15**(2020)** 2961 – 2972, doi: 10.20964/2020.04.05

International Journal of
ELECTROCHEMICAL
SCIENCE
www.electrochemsci.org

Effect of Surface Roughness on Copper Corrosion in Simulated Beishan Groundwater, China

Minglei Hu[1], *Wei Zhang*[2,*], *Xianhe Shang*[1], *Jie Wen*[1], *Zhenjiang Zhao*[2], *Bingxuan Qiao*[2], *Decheng Kong*[2], *Chaofang Dong*[2,*]

[1] China Nuclear Power Operation Management Co., Ltd, Zhejiang 314300, China
[2] Institute for Advanced Materials and Technology, University of Science and Technology Beijing, Beijing 100083, China
[*]E-mail: huml@cnnp.com.cn, 15201461811@163.com

Received: 8 October 2019/ *Accepted:* 4 December 2019 / *Published:* 10 March 2020

The simulated Beishan groundwater of preselected area for high level nuclear waste disposal was prepared and the effect of surface roughness on corrosion behavior of copper was characterized by potentiodynamic polarization, immersion tests and scanning electrochemical microscope (SECM) measurements. It was found that as the surface roughness increased, the corrosion activity of copper was accelerated. Meanwhile, the corrosion current decreased by around 85.6% as the roughness values decreased from approximately 2.34 μm to 0.33 μm and there was no much change after further polishing. The SECM results showed that the corrosion current near the scratch was much higher than the smooth region, which meant a high oxygen consumption in scratch positions and indicated that surface irregularities led to a preferential dissolution and corrosion.

Keywords: Copper corrosion; Beishan groundwater; Surface roughness; Scanning electrochemical microscope; Nuclear waste disposal.

1. INTRODUCTION

Copper has been chosen to be a canister candidate metal in various High-Level Nuclear Waste (HLNW) isolation programs (e.g., those in European countries) [1-5], due to its thermodynamic immunity as regard to corrosion problems in pure, anoxic groundwater. However, the canisters in the granitic repositories will be placed at a depth of 500−1000 m underground, and for which the designed service life will be 10^5 to 10^6 years [6-9]. The ground water contains aggressive species that are known to activate copper toward corrosion, especially chloride ion, sulfur ion and nitrate ion. In general, the containers would be produced using cast iron as an inner layer for structural support and pure copper as an outer layer for corrosion protection (the thickness will be in a range from 30 to 50 mm). During the

storage stage, the canister itself will experience various environmental scenarios, an oxic environment lasts for the first few decades, and then an anoxic period after the initially trapped oxygen has been consumed [10-12].

In China, works on repository selection has been conducted since 1985 [13, 14]. The primary efforts were conducted on the Beishan area in Gansu Province of northwestern China, which contains many granite intrusions [15, 16]. For corrosion issue, the primary information about the water chemistry parameters should be obtained, including the pH value, dissolved oxygen content and chemical components concentration. There were 19 drill holes around 500~80 0m deep had been completed since 2000 and many environmental parameters had been obtained [17, 18]. It's a huge project to build such a deep repository and the long-term corrosion issue will also be a big challenge. It's known that the possibility of pitting in the passive film depends on the concentration and distribution of defects in the passive film as well as the electrolyte composition, temperature and the surface state. Frequently, corrosion initiates from a preferential dissolution at surface irregularities with a nanometer dimension [19-24]. More recently, scanning electrochemical microscope (SECM) technique was applied to investigate the local corrosion processes at the micro scale level [25-28] and this can be also used to study about the surface roughness effect on corrosion issues.

Since the nuclear waste disposal was an economical and security issue, there is very necessary to investigate the surface roughness effect on copper corrosion in Beishan groundwater. Actually, corrosion problems lead to US$4 trillion financial loss each year globally because of corrosion damage and corrosion protection investment, thus we must pay more attention to the corrosion issues. In our work, a series of electrochemical measurements were conducted with different surface states of copper via mechanical polishing, including potentiodynamic polarization curves, immersion tests and SECM experiments. This research will provide some guidance and reference significances in the surface treatment of copper canister in our future design.

2. EXPERIMENTAL DETAILS

2.1 Material ad solution

The solutions were prepared using simulated the Beishan groundwater, and Table 1 showed the concentrations of chemical components in Beishan groundwater under 600 meters [14]. A solution of pH = 8.4 was established with sodium hydroxide solution. In order to avoid atmospheric oxygen, all experiments were conducted under continuous nitrogen purging and the working electrode in this work was used with pure copper.

Table 1. The concentrations of main chemical components in Beishan groundwater under 600 meters [14].

Chemical Components	NaCl	$CaSO_4$	Na_2SO_4	$MgSO_4$	$NaHCO_3$	$NaNO_3$	KCl
Concentrations (mM)	35	5.5	5.2	2.4	1.6	0.5	0.5

2.2 Electrochemical measurements

Potentiodynamic polarization (PDP) curves were conducted using a three-electrode cell: a Pt plate as the counter electrode (CE), and a saturated calomel electrode (SCE) as the reference electrode (RE). Before PDP, the working electrode was cathodically polarized at −0.5 V_{SCE} for 5 min to remove air-formed oxidation products, and then PDP was commenced from the negative potential (−0.5 V_{SCE}) to positive potential (0.1 V_{SCE}) with a scanning rate of 0.1667 mV/s. Immersion tests were performed in anaerobic groundwater for 7 days and the surface morphology was observed by scanning electron microscope (SEM). The SECM resolution is approximately 100 nm with linear encoders on all directions independently. SECM experiments were conducted in a conventional four-electrode electrochemical cell with a Pt microelectrode (around 15 μm), a SCE serves as RE, a Pt wire is a CE, and the pure copper.

3. RESULTS AND DISCUSSION

3.1. Surface topography of copper specimens after different surface treatments.

Surface roughness problem can be involved in many processing methods, such as improper cutting and welding, which would have a great effect on the future performance of the workpieces. Figure 1 showed the surface topography of copper specimens fabricated by various emery papers grounding methods: (a) 60#, (b) 150#, (c) 400#, (d) 1000# and (e) 4000#, and (f) 1 μm diamond paste polishing, respectively. Clearly, there were obvious parallel scratches induced by surface finishing. With the finishing condition becoming finer, the copper surface became smoother and the surface scratches were less obvious in the field of vision. More than ten sites were selected on each specimen to measure the roughness using the laser confocal microscope, statistical surface roughness results are displayed in Figure 2. Obviously, the surface roughness of the specimens decreased when the surface finishing became fine. The specimen ground with 150# paper had a surface roughness of 1.09 ± 0.19 μm, and it decreased to about 0.15 μm after polished by 1 μm diamond paste.

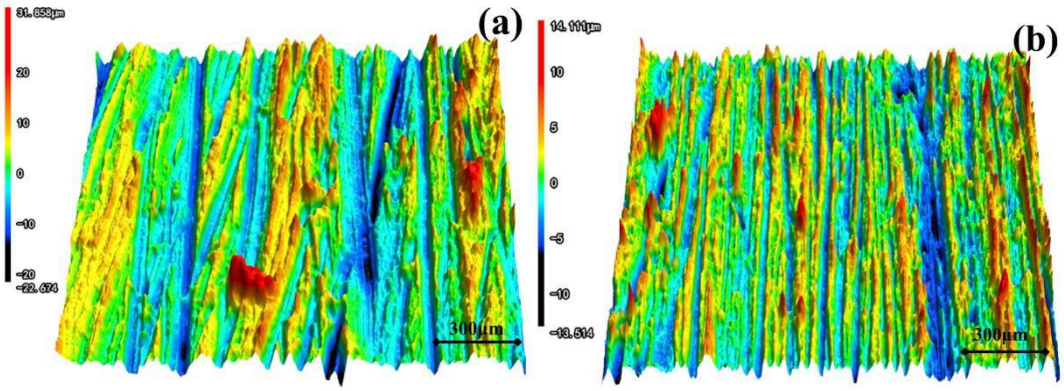

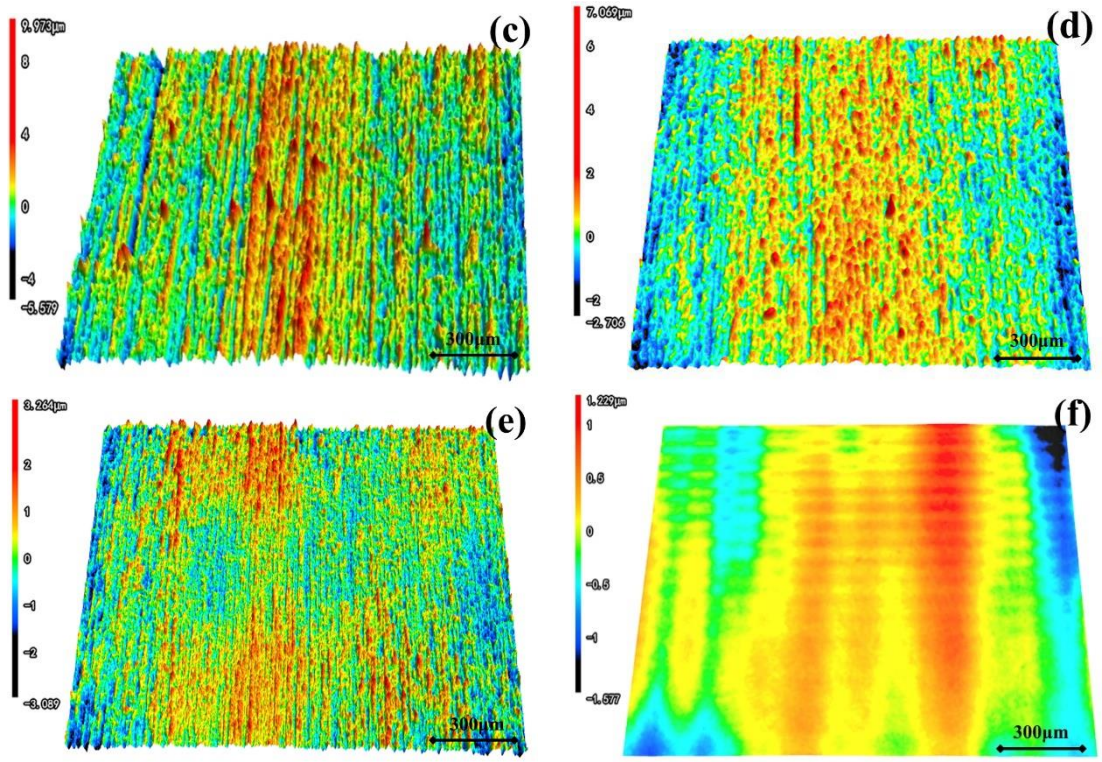

Figure 1. The surface topography of copper specimens prepared with various emery papers grounding methods: (a) 60#, (b) 150#, (c) 400#, (d) 1000# and (e) 4000#, and (f) 1 μm diamond paste polishing, respectively.

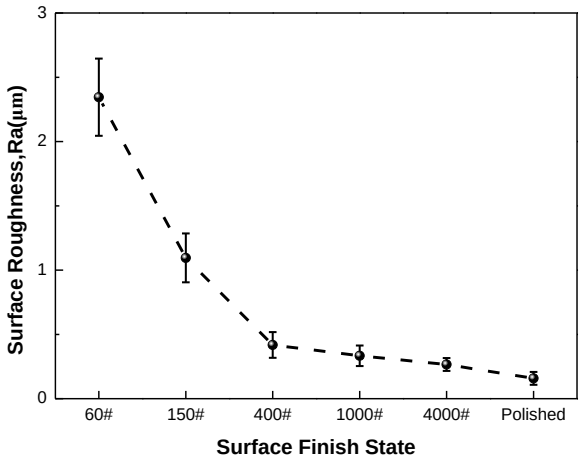

Figure 2. The statistical results of surface roughness with different surface finish states calculated by laser confocal microscopy.

It can be seen from the potentiodynamic polarization curves of copper in deaerated simulated Beishan groundwater displayed in Figure 3, there was no much difference for anodic process between different surface states and the copper electrodes came directly up to the anode dissolve activation state with the applied potential increased over the null-current potential. However, surface roughness did have an obvious influence on the cathodic reaction, since continuous nitrogen purging of the solution during our tests, the cathodic current mainly represented the amount of hydrogen evolution and the more rough the surface was, the more amount of hydrogen evolution was, which might be attributed to the more sites

for hydrogen evolution reaction or much easier for hydrogen evolution reaction at bulged sites. The Tafel fitting results are listed in Table 2 and it can be seen that the corrosion potentials did not have much difference for different surface conditions and were around -0.26 V_{SCE}. The cathodic Tafel slope was significantly larger than the anodic Tafel slope (approximately 5 times), which indicated that the oxygen reduction reaction dominated the primary corrosion process in our work. The corrosion current density decreased with the copper surface became smoother, which meant the higher corrosion resistance for copper with less roughness. The corrosion current density decreased by around 85.6% as the roughness values decreased from approximately 2.34 μm (60 #) to 0.33 μm (1000 #) and there was no much change after further polishing.

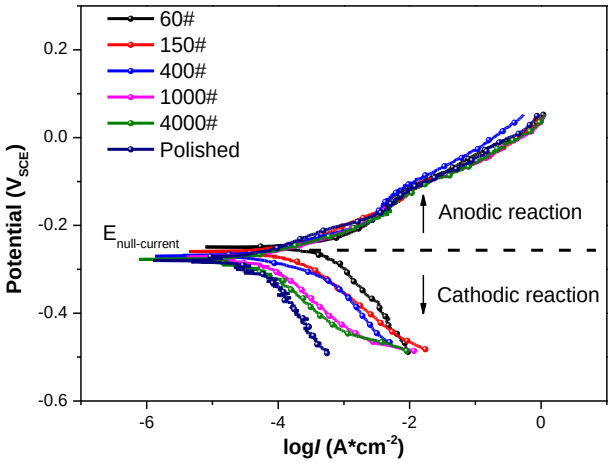

Figure 3. Potentiodynamic polarization curves of copper with different surface treatments in deaerated simulated Beishan groundwater, the scanning rate was 0.1667 mV/s.

Table 2. The corrosion potential, corrosion current density, Tafel slope values of the potentiodynamic polarization curves in Figure 3.

Surface conditions	Corrosion potential (V_{SCE})	Current density (μA cm^{-2})	Anodic Tafel slope (mV)	Cathodic Tafel slope (mV)
60#	-0.254 ± 0.015	0.35 ± 0.01	58 ± 4	280 ± 17
150#	-0.268 ± 0.011	0.10 ± 0.01	62 ± 5	327 ± 21
400#	-0.276 ± 0.022	0.06 ± 0.006	59 ± 6	311 ± 22
1000#	-0.262 ± 0.016	0.06 ± 0.005	67 ± 3	288 ± 15
4000#	-0.287 ± 0.023	0.05 ± 0.005	60 ± 4	299 ± 19
Polish	-0.273 ± 0.017	0.04 ± 0.005	59 ± 4	318 ± 26

3.2 Immersion tests

Specimens with different surface roughness were immersed in anoxic Beishan groundwater for 7 days and the surface morphologies are displayed in Figure 4. It can be clearly seen that a nonuniform

distribution of the corrosion products existed on the more rough surface,and this should be ascribed to the surface irregularities with more ledges, and kinks. Similar results were also found in others' studies [31]

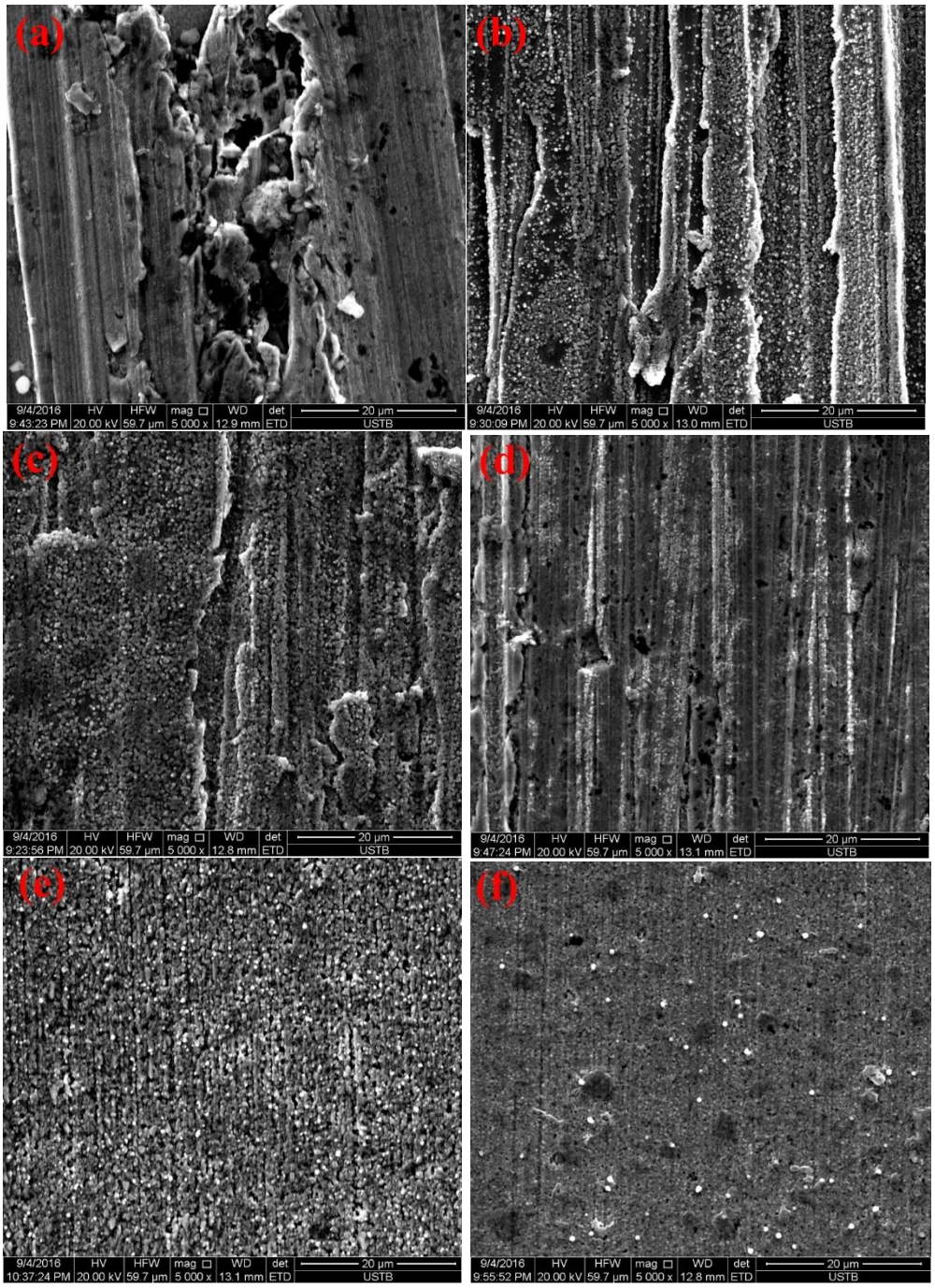

Figure 4. The surface morphologies of copper with different surface roughness after immersion in Beishan groundwater for 7 days: (a) 60#, (b) 150#, (c) 400#, (d) 1000# and (e) 4000# papers grounding, and (f) 1 μm diamond paste polishing, respectively.

Meanwhile, the corrosion products became more continuous and compact with the surface got more smooth and eventually completely covered on the substrate, which would logically provide a better

protection from further corrosion. And the main corrosion product of copper in Beishan groundwater was Cu_2O, as well as little chloride and hydrosulfate.The corrosion products were similar with the products of atmospheric corrosion for copper or copper alloys [32, 33].

3.3 SECM measurements

The testing electrolyte was the prepared Beishan groundwater and the solution was under continuous nitrogen purging of the cell and all experiments were conducted at ambient temperature. The sample we prepared is displayed in Figure 5, we can see two different depths of scratches simulated different roughness heights, of which the shallow and deep scratches marked by the red dotted line were about 27±1 and 43±3 μm, respectively.

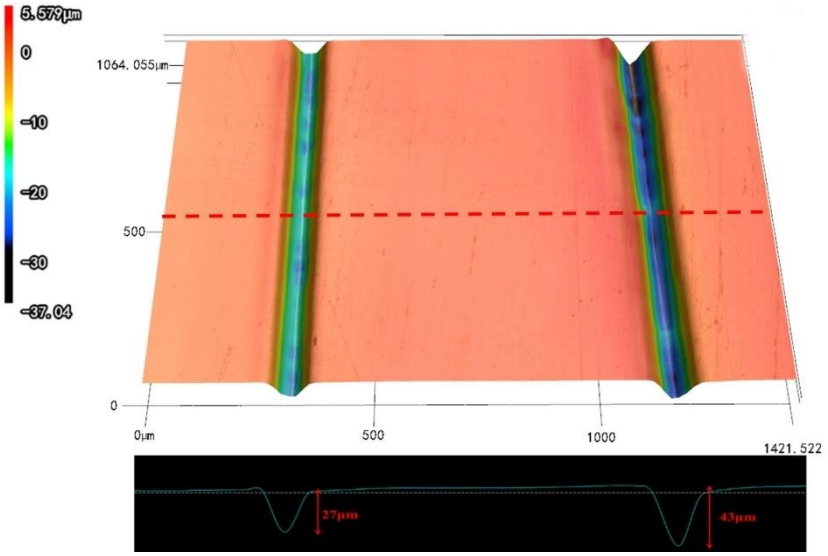

Figure 5. The copper sample with two different depths of scratches, one was 27 μm depth and the other was 43 μm, respectively.

Figure 6 (a) displays the cyclic voltammogram result of the Pt micro-electrode in the groundwater solution and it was evident that there was a plateau current ranging from -0.75 V_{SCE} to -0.35 V_{SCE} and oxygen content here is very low. Thus, the tip potential can be set at -0.55 V_{SCE} to in our solution situation. The approaching curve was displayed in Figure 6 (b), the tip now was approximately 85.4 μm far away from the copper surface and the tip was subsequently retracted around 70.4 μm, resulting in a 15 μm tip-sample distance.

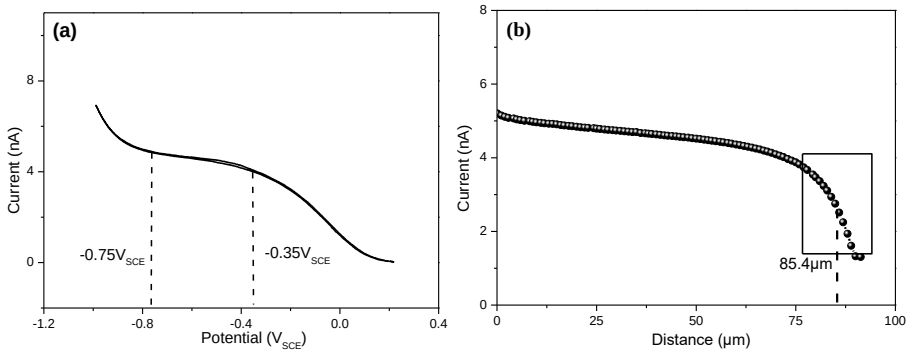

Figure 6. (a) Cyclic voltammogram results of the Pt-microelectrode in simulated Beishan groundwater (pH = 8.4) solution, scan rate: 20 mV$_{SCE}$ s^{-1}; (b) Approach curve: the variation of current with the tip-substrate distance.

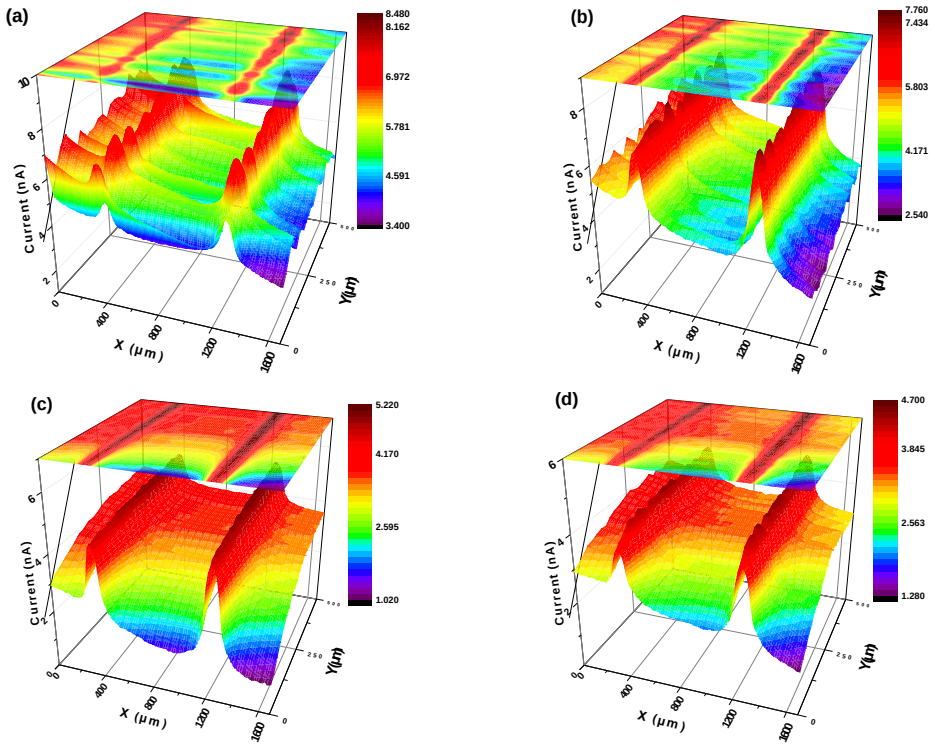

Figure 7. SECM image of different depths of scratches on copper surface in simulated Beishan groundwater (pH = 8.4) solution: (a) 4, (b) 12, (c) 24, (d) 48 h. Tip potential: –0.55 V$_{SCE}$, scan area: 1680μm × 500μm, scan rate: 15 μm s^{-1}, current unit: nA.

Figure 7 shows the SECM image of different depths of scratches on copper surface in simulated Beishan groundwater (pH = 8.4) solution: (a) 4, (b) 12, (c) 24 and (d) 48 h, respectively. It can be clearly seen that the current near the scratch was much higher than the smooth region, which meant a high oxygen consumption in scratch positions and indicated that surface irregularities lead to a preferential dissolution [34]. In acidic environments, the hydrogen evolution reaction is the major cathodic partial reaction, whereas, in near neutral or alkaline solutions, the oxygen reduction reaction has to be regarded as the major cathodic reaction due to the high solubility of oxygen in aqueous electrolytes [35]. This current difference was much clearer as displayed in Figure 8 (a), Figure 8 (b) displays the current difference between the scratch and the near smooth region with immersion time and we can see the

current difference of deep scratch was larger than the shallow counterpart, and that further indicated the corrosion would be more serious at those more roughness sites. The corrosion current difference increased at first then decreased, which represented the corrosion process that the corrosion was first accelerated due to the scratch that separated a high and a low oxygen consumption area, and then decreased simply indicated a protective effect of the surface passive film or corrosion products. Moreover, Li et al. [36] pointed out that it was easier for electrons in the vicinity of a peak to escape than those in a valley site, therefore, the peak would be corroded preferentially. They also confirmed that the electron work function fluctuation would increase with the increasing surface roughness and may also promote the formation of corrosion self catalytic cell that could further accelerate the corrosion process of a rough area.

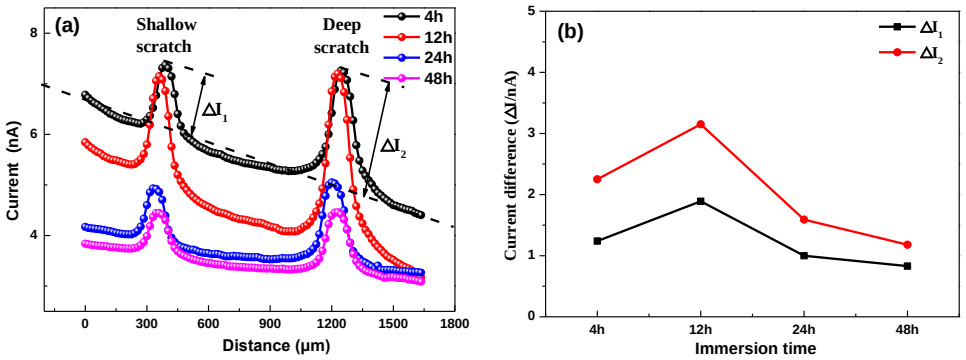

Figure 8. (a) the linear scan image of different depths of scratches on copper surface in simulated Beishan groundwater (pH = 8.4) solution; (b) the current difference between the scratch and the near smooth region.

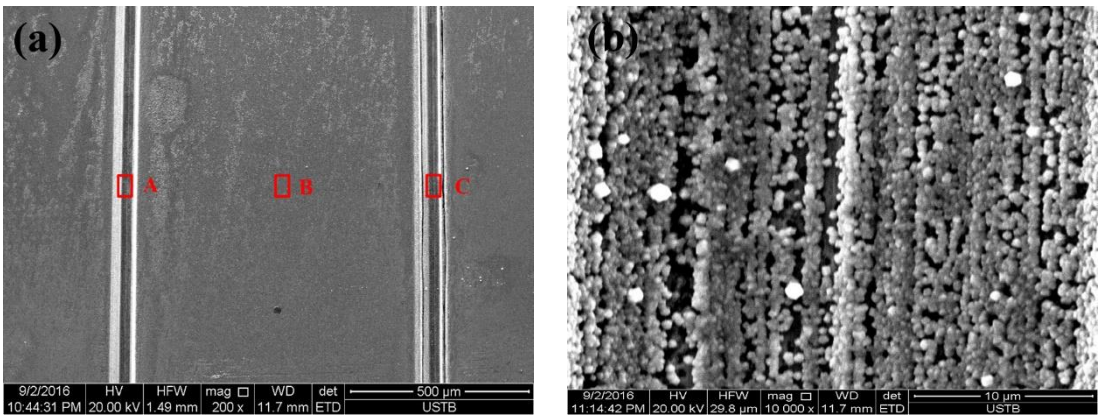

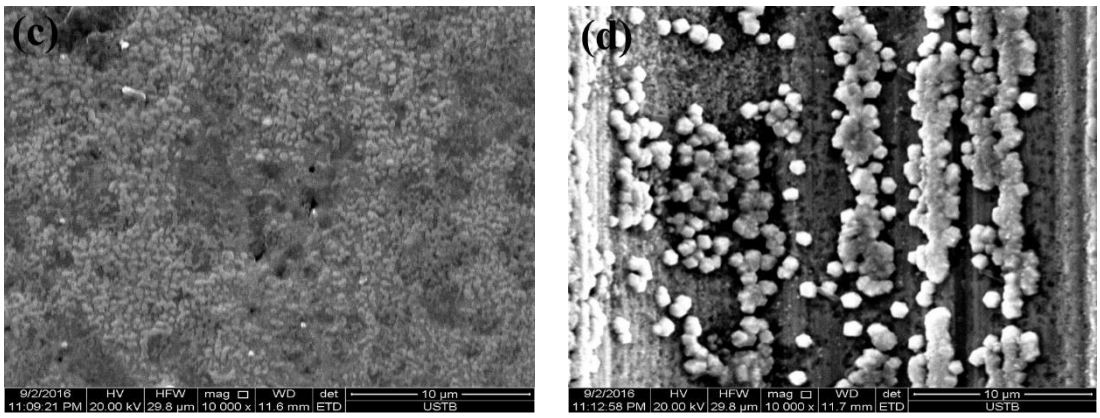

Figure 9. The surface morphology of copper after 48h SECM experiment in simulated Beishan groundwater (pH = 8.4) solution: (a) the whole morphology, (b) A-area with shallow scratch, (c) B-area without scratch, (d) C-area with deep scratch.

Figure 9 shows the surface morphology of copper after 48-h SECM experiment in simulated Beishan groundwater (pH = 8.4) solution: (a) the whole morphology, (b) A-area with shallow scratch, (c) B-area without scratch, (d) C-area with deep scratch. It was obvious that the B-area without scratch was the most compact and the corrosion product in A-area with shallow scratch was more continuous than the C-area with deep scratch, and loose and porous products irregularly covered on the scratch surface at C-area, which indicated that the edges and corners area was more likely to corrode and no further protection. Similar results were also found on stainless steels [37] that metastable pits or stable pits start to grow at the rough surface sites, and the smoother the surface, the higher metastable pitting potential values. In general, pitting susceptibility and general corrosion rate all increased with the increase in the surface roughness of stainless steels [38-40]. A similar phenomenon has also been reported for other materials, such as copper and magnesium alloys [41]. Thus, in the design of the copper canister for the high-level nuclear waste disposal, surface modification technique should be carefully evaluated in the future, methods such as sand blasting, micro-arc oxidation, electrochemical deposition, alkali-acid-heat treatment, can be chosen according to the characteristics of the components.

4. CONCLUSIONS

In our study, an appropriate groundwater system was chosen according to the environments of the Beishan high level nuclear waste repository and the effect of surface roughness on corrosion behavior of copper, a candidate canister material, was characterized by potentiodynamic polarization, immersion tests and SECM measurements. The results showed that the corrosion resistance decreased as the surface roughness increased, and the corrosion current decreased by around 85.6% as the roughness values decreased from 2.34 μm to 0.33 μm and there was no much change after further polishing. The SECM results showed that the current near the scratch was much higher than the smooth region, which meant a high oxygen consumption in scratch positions and indicated that surface irregularities led to a preferential dissolution. Moreover, the corrosion products became more continuous and compact with more smooth surface, which would further protect the substrate from corrosion. Thus, a good surface

condition for copper canister was very essential for a long service-life disposal ad this work can provide very necessary engineering data for future canister design.

ACKNOWLEDGEMENTS
The authors thanks for the financial support by National Key Research and Development Program of China (No. 2017YFB 0702300).

References

1. D.G. Bennett and R. Gens, *J. Nucl. Mater.,* 379 (2008) 1.
2. D.C. Kong, A.N. Xu, C.F. Dong, F.X. Mao, K. Xiao, X.G. Li and D.D. Macdonald, *Corros. Sci.,* 116 (2017) 34.
3. D.C. Kong, C.F. Dong, X. Wei, C. Man, X.W. Lei, F.X. Mao and X.G. Li, *Electrochim. Acta,* 292 (2018) 817.
4. D.C. Kong, C.F. Dong, X.Q. Ni, A.N. Xu, C. He, K. Xiao and X.G. Li, *Mater. Corros.,* 68 (2017) 1070.
5. D.C. Kong, A.N. Xu, C.F. Dong, F.X. Mao, K. Xiao and X.G. Li, *J. Mater. Eng. Perform.,* 26 (2017) 1741.
6. F. King. *JOM,* 66 (2014) 526.
7. A. Hedin. *Math. Geosci.,* 40 (2008) 619.
8. C.F. Dong, F.X. Mao, S.J. Gao, S. Sharifi, P. Lu and D.D. Macdonald, *J.Electrochem.Soc.,*163 (2016) 707.
9. S.A. Tiren, P. Askling and S. Wanstedt. *Eng. Geol.,* 52 (1999) 319.
10. J.M. Smith, J.C. Wren and M. Odziemkowski. *J. Electrochem. Soc.,* 154 (2007)431.
11. D.C. Kong, C.F. Dong, M.F. Zhao, X.Q. Ni, C. Man and X.G. Li, *Corros. Eng. Sci. Tech.,* 53 (2018) 122.
12. D.C. Kong, C.F. Dong, A.N. Xu, C. He and X.G. Li, *Corros. Eng. Sci. Tech.,* 52 (2017) 188.
13. X.G. Zhao, J. Wang and M. Cai. *Eng. Geol.,* 163 (2013) 26.
14. X.G. Zhao, J. Wang and F. Chen. *Tectonophysics,* 683 (2016) 124.
15. W.M. Ye, Y.G. Chen and B. Chen. *Eng. Geol.,* 116 (2010) 12.
16. Y. He, Y.G. Chen and W.M. Ye. *Environ. Earth Sci.,*75 (2016) 1.
17. F. Xiao, J. Wang and Y.H. Guo. *Uranium Geol.,* 27 (2011) 185.
18. Y.H. Guo, J. Wang and Z.M. Wang. *Uranium Geol.,* 26 (2010) 46.
19. D.C. Kong, X.Q. Ni, C.F. Dong, X.W. Lei, L. Zhang, C. Man, J.Z. Yao and X.G. Li, *Mater.Design*, 152 (2018) 88.
20. D.C. Kong, X.Q. Ni, C.F. Dong, L. Zhang, C. Man, J.Z. Yao, K. Xiao and X.G. Li, *Electrochim. Acta*, 276 (2018) 293.
21. Z.Y. Liu, X.G. Li and Y.F. Cheng, *Electrochim.Acta,* 56 (2011) 4167.
22. Z.Y. Liu, X.G. Li and Y.F. Cheng, *Electrochim.Acta,* 60 (2012) 259.
23. Y.F. Cheng and J.L. Luo, *J.Electrochem.Soc.,* 146 (1999) 970.
24. D.C. Kong, C.F. Dong, X.Q. Ni and X.G. Li, *Npj Mater. Degrad.,* 3 (2019) 24.
25. A.O. Okunola, T.C. Nagaiah and X. Chen, *Electrochim. Acta,* 54 (2009) 4971.
26. Y. G. Garcia, J.M.C. Mol and T. Muselle, *Electrochem. Commun.,* 13 (2011) 169.
27. S.J. Gao, C.F Dong and H. Luo, *Electrochim. Acta*, 114 (2013) 233.
28. D.C. Kong, C.F. Dong, Z.R. Zheng, F.X. Mao, A.N.Xu, X.Q. Ni, C. Man, J.Z. Yao, K. Xiao and X.G. Li, *Appl. Surf. Sci.,* 440 (2018) 245.
29. B.R. Hou, X.G. Li, X.M. Ma, C.W. Du, D.W. Zhang, M. Zheng, W.C. Xu, D.Z. Lu and F.B. Ma, *Npj Mater.Degrad.,*4 (2017) 1.

30. X.G. Li, D.W. Zhang, Z.Y Liu, Z. Li, C.W.Du and C.F. Dong, *Nature*, 527 (2015) 441.
31. X.N. Suo, C. Guo, Li Wang and D.C. Kong, *Int. J. Electrochem. Sci.,* 14 (2019) 826
32. D. C. Kong, C. F. Dong, Y. H. Fang, K. Xiao, C. Y. Guo, G. He and X. G. Li, *J. Mater. Eng. Perform.*, 25 (2016) 2977.
33. D.C. Kong, C.F. Dong, X.Q. Ni, C. Man, J.Z. Yao, K. Xiao and X.G. Li, *Appl. Surf. Sci.*, 455 (2018) 543.
34. M. Stratmann and J. Müller, *Corros. Sci.,* 36 (1994) 327.
35. Y. Miyata and S. Asakura, *Corros. Sci.,* 44 (2002) 589.
36. W. Li and D.Y. Li, *Acta Mater.*, 54 (2006) 445.
37. T. Hong and M. Nagumo, *Corros. Sci.,* 39 (1997) 1665.
38. Y. Zuo, H. T. Wang and J. P.Xiong, *Corros. Sci.,* 44 (2002) 25 .
39. A. Shahryari, W. Kamal and S. Omanovic, *Mater. Lett.,* 62 (2008) 3906.
40. D.C. Kong, C.F. Dong, X.Q. Ni, L. Zhang, H. Luo, R.X. Li, L. Wang, C. Man and X.G. Li, *Appl. Surf. Sci.*, 144 (2019) 495.
41. R. Walter and M. B. Kannan, *Mater. Design,* 32 (2011) 2350.